2022

Multi-Objective Optimization of Battery Electric Vehicle Thermal Management System Operation

Tyler Shelly

Justin A Weibel

Davide Ziviani

Eckhard Groll

A Comprehensive Framework for Lifetime Battery Aging Assessment Considering Electric Vehicle Driving Behavior and Ambient Conditions

Marie Rae Shelly[1]*, Justin A. Weibel[1], Davide Ziviani[1], Eckhard A. Groll[1]

[1]Purdue University, School of Mechanical Engineering,
West Lafayette, IN, USA

tshelly@purdue.edu, jaweibel@purdue.edu, dziviani@purdue.edu, groll@purdue.edu

* Corresponding Author

ABSTRACT

The optimization of battery electric vehicle thermal management systems (BEV TMS) operations should consider several performance objectives including energy efficiency, battery aging, system range, and cabin comfort. Studies investigating comprehensive boundary and initialization conditions are necessary to understand the impact of BEV TMS design, construction, and operation on these performance objectives. In this work, a dynamic model of a TMS incorporating waste heat recovery (WHR) from power electronics and the battery is used to investigate battery aging within a holistic boundary condition and initialization framework that accounts for vehicle conditioning before, during, and after a scheduled test. Parametric investigations are performed accounting for the conditioning and dwell of the vehicle prior to testing cycles, ambient conditions averaged across the United States, and lifetime data of typical light-duty vehicle behavior. These are then presented inside a binned framework established for gauging lifetime impact of the thermal management system on battery aging as a function of drive cycle intensity, the vehicle resting period, and ambient temperature.

1. INTRODUCTION

Battery electric vehicle (BEV) thermal management systems (TMSs) require design, optimization, and construction across multiple scales to ensure they achieve optimal performance and meet consumer demands. Global warming (IPCC, 2022), decarbonization, and energy savings are a few of the main drivers (VTO, 2021) of wider adoptions of these vehicles, while consumer concerns remain a bottleneck. Typical concerns include vehicle range, safe and reliable operation in a variety of climates, and the lifetime performance of battery modules. These aspects are often addressed separately with investigations focused on optimizations of alternate system architectures or control strategies to increase vehicle range (Titov & Lustbader, 2017), study of heating, ventilation, and air conditioning (HVAC) for extreme climates (Yu, et al., 2019), and the aging characteristics of battery cells (Arenas, et al., 2015). Rarely are all such criteria investigated in an integrated fashion using a comprehensive BEV TMS model subject to real-world use cases. In addition, most of the experimental investigations of such systems simplify the interactions between the system components (*e.g.*, power electronics, HVAC, battery) and their surrounding environment. For example, such simplifications include assumptions of isothermal conditions for battery aging (Jafari, et al., 2018) (Li, et al., 2019), lumped temperature cells in thermal network representations (Du, et al., 2020), or treating power electronics and battery loads as constant or negligible (Zhang, et al., 2018) (Titov & Lustbader, 2017). However, it is important to consider these additional complexities as the conditioning loads for battery modules, cabin HVAC, and power electronics can impose additional power consumption and increase overall current throughput (Ah) for the battery pack per drive cycle. The temperature response of the battery pack is particularly critical to consider as batteries are known to age poorly under high- and low-temperature conditions.

The purpose of this work is to use a holistic BEV TMS model which encompasses the power electronics, cabin environment, and battery to predict the lifetime aging of the vehicle battery pack as a function of ambient conditions, assumed drive cycle, and the resting period of the vehicle. This encompasses a novel lifetime preconditioning framework which considers the thermal initialization of the vehicle under conditions representative of end use. The model is then used to predict battery lifetime aging as a function of vehicle resting period, drive cycle intensity, and ambient temperature.

2. MODELING FRAMEWORK

The modeling framework described herein is the product of several years of research and as such the authors' past work is referenced for detailed descriptions of the TMS model (Shelly , et al., 2020), system operation and range optimization (Shelly, et al., 2021), comparison of TMS architectures (Shelly , et al., 2021), and establishment of a co-simulation framework for investigating high-fidelity simulation of the battery modules within the reduced-order TMS simulations (Shelly, et al., 2022). Sections 2.1-2.3 below offer brief overviews of the core elements of the modeling framework for clarity; relevant additions or modifications to the simulation environment are noted in the corresponding sections. Section 2.4 introduces the novel approach developed for calculating lifetime aging of the battery based upon imposed boundary conditions realistic for light-duty vehicles across the United States.

2.1 Thermal Management System Model

The TMS model is implemented in Dymola (Dassault Systèmes, 2019) using the Modelica programming language. This model utilizes TIL libraries from TLK (TLK-Thermo GmbH) for common definitions of thermal system components based upon the homogenous equilibrium model. The TMS system analyzed comprises several typical vapor compression cycle components and is configured to allow for waste heat recovery (WHR) via a series of flow control valves, as illustrated in Figure 1. Beginning at the compressor, C1, superheated vapor is compressed to a high-pressure state. This vapor is then sent to the front-end heat exchanger (HX) which takes in air from the environment and condenses the superheated vapor to a subcooled liquid state at the outlet of the condenser. From there, the subcooled liquid is split between cabin HX and battery HX. Valve V1 controls inlet superheat to the compressor, while valve V2 controls the inlet temperature to the battery cold plate. Valve V3 controls the mode of the heat pumping cycle, allowing it to change between heating and cooling function depending on the ambient temperature and component temperature setpoints. A water glycol coolant network routes throughout the BEV TMS to allow for waste heat recovery from the power electronics to be used for battery or cabin heating, as controlled by valves V4 and V5. Finally valve V6 allows for proportional control of the cabin or battery temperature via power electronics waste heat recovery, or for cooling of the power electronics during a heating scenario. A detailed description of this system is provided in the authors previous work (Shelly, et al., 2021).

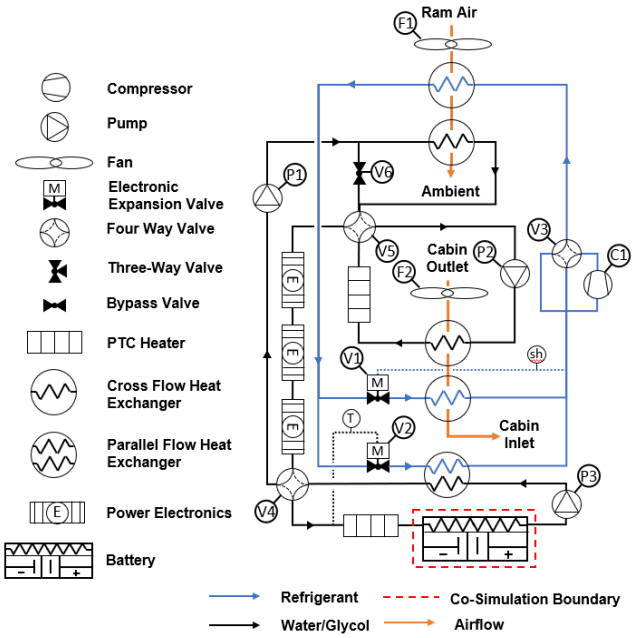

Figure 1: Waste heat recovery (WHR) battery electric vehicle (BEV) thermal management system (TMS) with arrowheads indicating the flow direction in cooling model.

2.2 Battery Module Model

The battery pack geometry and thermophysical properties, listed in Table 1, are for a pack with 108 cells in series and 16 in parallel (108S 16P).

Table 1: Battery physical parameters based upon a 108S 16P pack configuration with each of the modules lined up side-to-side.

Parameter	Value	Unit
$length$	0.69	m
$width$	3.86	m
$height$	0.17	m
$mass$	661.82	kg
ρ_{cell}	0.69	kg/m^3
$c_{p,cell}$	3.86	kJ/kg-K

Electrically, the battery is represented as a single internal resistance (R) and open circuit voltage (OCV) which is termed an equivalent circuit. Power demand from the overall system then imposes current through the battery pack based on the OCV which determines the ohmic heating losses inside of each battery cell based on each cell's internal resistance. The battery state of charge (SOC) is then found via coulomb counting which integrates the imposed current on the battery. Aging parameters for the battery cell are defined based on the temporal change in battery capacity, termed capacity loss, and increase in internal resistance, termed power fade. Governing equations for the thermophysical properties discussed above are taken from an open literature source (Arenas, et al., 2015) which captures its aging and thermal performance as a function of temperature and current throughput over time. These parameters are not available at low temperatures below 20 °C, and therefore are normalized to allow simulation of such cases; an extensive review of available reduced-order battery models and a details description of the implementation of the equivalent circuit model are available in our prior work (Shelly, et al., 2021). The battery module, shown in Figure *2*, is implemented into the COMSOL[1] modeling platform and is arranged in a straight flow configuration with a cold plate running along the bottom of the module. Thermal management of the battery using the water/ethylene glycol loop is accomplished with a cold plate with liquid flow along the cells from single inlet to a single outlet. The cold plate interfaces with thermally conductive fins interspersed between parameterized battery cells for indirect cooling. Thermal interface materials (TIMs) are represented as contact resistances with a representative value of 300×10^{-6} m^{2}K/W (Cui, et al., 2019) at each contacting surface within the battery pack. These surfaces are indicated in Figure 2 between the battery cell and fin, and between the fin and the cold plate. The coolant is a water ethylene glycol 50/50 mixture which is commonly used to protect against freezing inside such systems even at low ambient temperatures.

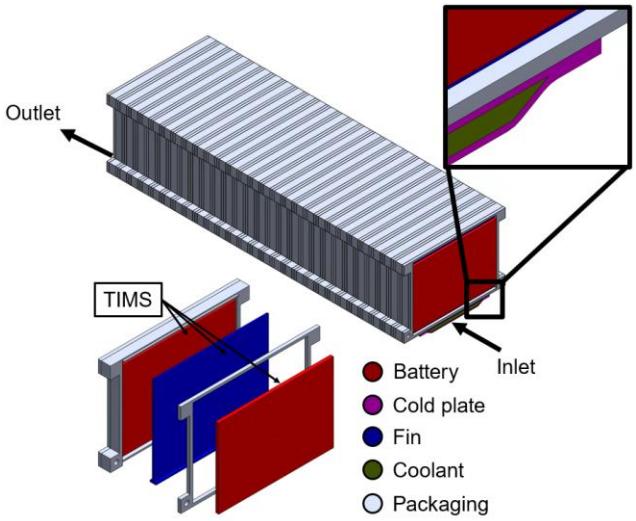

Figure 2: Battery module defined with 108 cells in series and 1 in parallel (108S, 1P)

[1] Multiphysics®, C. (2021). COMSOL Multiphysics® v. 5.6. Stockholm, Sweden: COMSOL AB. Retrieved from www.comsol.com

The packaging structure surrounding the cells approximates the structure necessary to hold the battery pack together under mechanical pressure to ensure cell performance. The packaging material is assumed to be ABS plastic. Finally, the battery module shown is discretized into six cell groupings along the flow length of the module. Each cell grouping is made up of 18 cells.

2.3 Co-Simulation Procedure

The vehicle-level TMS model implemented in Modelica and the high-fidelity COMSOL battery module model are then co-simulated to accurately gauge the impact of boundary conditions and system operation on the battery thermal performance. Co-simulation allows the temperature field to be locally resolved in the battery pack for consideration of aging of each cell as a function of its placement in the battery module. The co-simulation procedure begins when both the TMS and battery models initialize and connect to a shared Java script server which coordinates the interfacing between of the two different simulation software platforms. As seen in Figure 3a once the simulation is started, point 1, Modelica will pass initial values of battery heat generation, coolant flow rate, and the inlet temperature of the coolant to the COMSOL simulation through the shared server. At this point 2, the battery module is simulated subject to these inputs up to point 3, where the simulation stops to synchronize with the server. The temperature field of the battery and outlet temperature of the module are then passed from COMSOL to back to Modelica, points 3 to 4, and gives the signal for the TMS simulation to proceed to prescribed time step, point 5, and begin this process again. This repeats until, at point 6, the TMS reaches the end-of-test time and sends a signal to stop the battery module simulation. The co-simulation process is governed by a network of controllers shown in Figure 3b. These are the charge-discharge controller, velocity profile controller, and adaptive time step controller. The charge discharge controller reads the current state of the battery and system and determines if the vehicle should be in a charging or discharging state. This is done by monitoring the battery pack state of charge and system control objectives. Once a control objective is reached this controller then outputs a charge-discharge binary value (CD), 0 or 1, which respectively indicate the vehicle state and controls the switching of system valving accordingly. Additionally, this controller outputs the demand current to the battery dependent on the vehicle mode. The velocity profile controller reads this CD value and controls the starting and stopping of the vehicle velocity profile at the correct instant. Once a charging state is detected, the vehicle is decelerated to stop and the cumulative time spent charging is recorded. This cumulative time spent charging is then subtracted from the input time to the velocity profile to ensure the vehicle begins at the point in the drive cycle where it stopped at before charging. This velocity profile controller also then handles the time indexing of the velocity profile at various time steps forward in time and passes these values to the adaptive time step controller. The adaptive time step controller adjusts the co-simulation time step based on the vehicle acceleration to ensure that fast acceleration events properly resolved during the co-simulation process. A full documentation of the control logic and characterization of co-simulation static and dynamic error can be found in the authors' previous work (Shelly, et al., 2022).

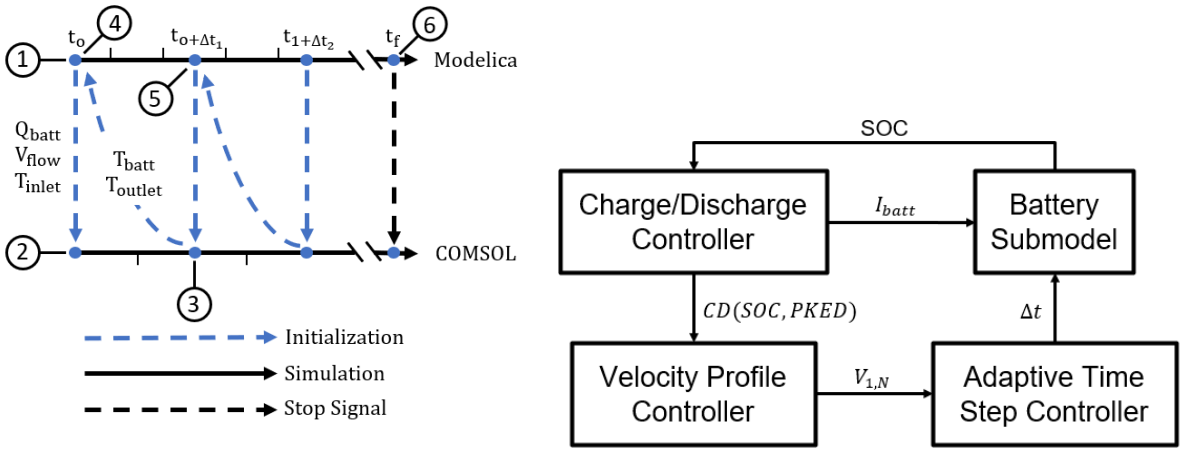

Figure 3: (a) Co-simulation time stepping scheme between Modelica (TMS model) and COMSOL (battery module model) and (b) overall co-simulation control process encompassing active charge-discharge control, velocity profile control, and adaptive time step control sensitive to vehicle acceleration and future events

2.4 Lifetime Battery Aging Prediction

2.4.1 Boundary Conditions:
To understand and gauge the impact of BEV usage on the aging performance of its battery, it the use cases considered must reflect how typical consumers operate light duty vehicles. This includes the initialization conditions of the vehicle before a drive cycle, how long and intensely the vehicle is driven, and how long the vehicle sits after a drive cycle. These conditions are available in open literature as the Transportation Secure Data Center (TDSC) collates consumer-level drive cycle data (Moniot, et al., 2021). This data includes vehicle velocity traces as a function of time as well as time the vehicle has spent resting. To categorize and rate the relative intensity of a vehicle velocity profile the metric of positive kinetic energy (PKED) (Moniot, et al., 2021) which is defined as the positive product of velocity and acceleration of the vehicle integrated over time as:

$$PKED = \int \begin{pmatrix} v*\frac{dv}{dt}, v*\frac{dv}{dt}>0 \\ 0, v*\frac{dv}{dt}<0 \end{pmatrix} dt \quad (1)$$

Per this PKED metric, the rating for severity of driving cycle monotonically increases with time and is influenced by velocity and positive acceleration components, while neglecting times of deceleration. The times when the vehicle is at rest, termed dwell periods, are categorized simply via the total duration over which the vehicle is at rest. The PKED and dwell period are then binned into three characteristic small, medium, or large PKED or dwell periods using data from the original sources (Moniot, et al., 2021), which were based on data from the thermal response of internal combustion engine vehicles (ICEVs). It is assumed that the once a vehicle begins a dwell period it begins charging as soon as it stops. The bins used are summarized in Table 2.

Table 2: Bin values for positive kinetic energy density (PKED) and dwell period.

Parameter	PKED	Unit	Dwell	Unit
Small	649.56	m^2/s^2	14	mins
Medium	2173.58	m^2/s^2	110	mins
Large	4456.32	m^2/s^2	360	mins

Finally, typical meteorlogical year (TMY3) data can be utilized to simulate under realitic regional or nationally averaged weather conditions. Relevant to the current student, ambient temperature and solar irradiatio are collated across national averages from original literature sources (Moniot, et al., 2021).

2.4.2 Thermal Initialization and Lifetime Simulation Matrix:
With nationally averaged driving behavior and ambient conditions defined, the simulation of the lifetime performance of a vehicle can be considered. The PKED and dwell bins allow for proper weighting of thermal system response and driver behavior as a function of the thermal system, its sizing, and the control strategies used to meet various temperature setpoint targets across these simulations. An approach is considered where a battery aging test cycle is assumed to occur after a 'conditioning cycle followed by a dwell period (Moniot, et al., 2021). Therefore, the thermal initialization of the vehicle before a test cycle (for which aging of the battery cell is calculated) is not a trivial soak at a uniform temperature, but rather is a complex system state that must be simulated in advance. To accomplish this the previously identified lifetime boundary conditions are applied as follows. First, the vehicle is soaked at the ambient temperature and its thermal system response to the conditioning cycle and dwell period is simulated for subsequent use as the initial thermal state of the vehicle at the beginning of the actual test cycle. Next is the actual test cycle simulation where battery aging is calculated as a function of its temperature and current throughput. These simulations are performed across a simulation matrix with the previously discussed bins for PKED, dwell period, ambient temperature, and solar irradiation. For simplicity, the solar irradiation is set to 0 W/m^2 for the thermal initialization simulations and constant at 200 W/m^2 for the aging simulations. However, the approach developed here could be trivially used to consider any other single value or distribution of solar irradiation of interest.

2.4.3 Reduced-Order Dwell and Aging Models:
To reduce overall simulation cost and increase the speed at which BEVs can be rated for battery aging, two reduced-order models are developed, the first of which is a reduced-order dwell period model. The dwell period model follows the conditioning cycle simulation throughout the dwell period. During the dwell periods, the vehicle is stationary with

all control systems turned off and only exchanges heat with the ambient. Simulation via the dynamic TMS model is unnecessarily detailed for these simple conditions and instead, only the temperature drift of the key vehicle control volumes (cabin and battery) and control tanks (battery and cabin coolant tanks) are tracked by the reduced-order dwell model. The coolant tanks are represented as spherical volumes while the cabin model itself is taken directly from the thermal system model. The heat transfer correlations are modified to natural convection correlations over the outside of the vehicle. The battery is treated as a single lumped thermal mass with heat transfer by natural convection to its surrounding. This is termed a reduced-order model (ROM) for the dwell period. Once the thermal initialization simulations are completed, aging simulations are performed to estimate battery aging across a single charge discharge cycle, which then should be extended across a lifetime of aging. However, because dynamic co-simulation of a vehicle over its entire lifetime is not practical as simulation times would be exceedingly long, a second ROM is introduced. This is an aging ROM which is developed to take the temporal temperature profile of the battery, now a function of current throughput after battery aging simulations are completed, and uses it to calculate aging and power fade as a function of temperature across a full lifetime of each discretized cell grouping ($Ah_{1-N}(T,t)$). Because this data is time synchronized and temperature is input as a function of current throughput, each battery bundle can be aged appropriately across the lifetime current throughput expected.

2.4.4 Solution Procedure:
Finally, the solution procedure for the lifetime battery aging assessment is summarized here and illustrated in Figure 4.

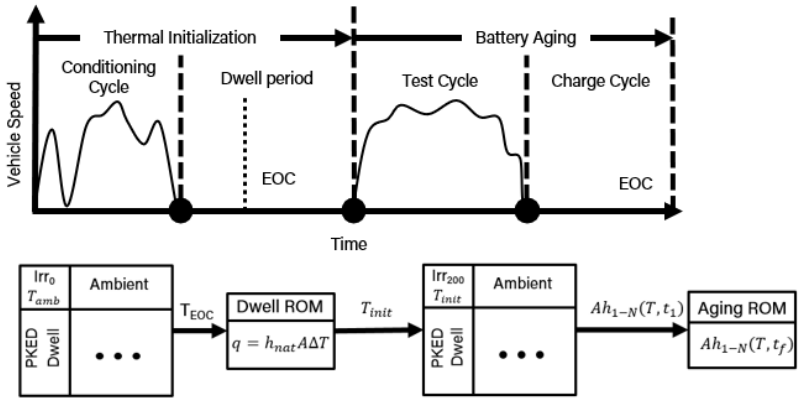

Figure 4: Schematic representation of the lifetime battery aging simulation framework as a function of PKED, dwell, ambient temperature, thermal initialization, and module construction. The lifetime simulation campaign (shown on the time trace at the top) is broken up into the thermal initialization portion, composed of a conditioning cycle and dwell period, and a battery aging portion, composed of a test cycle and charge cycle.

First is the thermal initialization where nationally averaged boundary conditions for ambient temperature and solar irradiance (T_{amb}, Irr) are input to a vehicle model assumed to be at an initial soak temperature of the ambient. The system response of key thermal system components is then simulated across a campaign of binned PKED and dwell periods. The vehicle is assumed to be charged at different rates depending on the length of the dwell period, specifically with the charging rate inversely proportional to the dwell period length, as reported in Table 3.

Table 3: Battery charging rate associated with each dwell period.

Dwell Period	C-Rate
Small	5 C
Medium	1 C
Large	1/3 C

Once the vehicle is co-simulated through the conditioning and the initial portion of the dwell cycle up to the end of charge (EOC) condition the co-simulation is stopped, and the temperatures of key thermal system components at the EOC (T_{EOC}) are input into the reduced-order dwell period model for each simulation point of the PKED, dwell, and ambient temperature matrix. Once complete a full thermal initialization of the system is completed, battery aging

simulations can begin with the system temperature calculated from thermal initialization (T_{init}). These are completed across the same binned simulation matrix as the thermal initialization simulations, but this time with updated initial thermal conditions. The vehicle is then simulated across a test cycle recording the temperature response as a function of the current throughput across the cycle, discretized for each cell grouping ($Ah_{1-N}(T,t)$). This temperature profile is then used in the battery aging reduced-order model to calculate lifetime impact, weighted across nationally averaged conditions for each point in the simulation matrix. This workflow is illustrated along the bottom of Figure 4.

3. RESULTS

Results are presented for the thermal initialization simulations and battery aging predictions under the subsequent test cycle simulations. Thermal initialization simulations assume an initial soaked condition and apply conditions representative of national light duty vehicle behavior and the ambient conditions these vehicles experience. This produces an initial temperature of key control volumes in the vehicle which is used to set the initial thermal state for test cycle simulations. Battery aging is then predicted according to these simulation results conditions across a single test and charge cycle. The results of the battery aging simulations are then used in an aging ROM which scales battery aging from this simulation linearly with lifetime current throughput.

3.1 Thermal Initialization Simulations

Figure 5 shows the battery temperatures with time during of two different thermal initialization simulations at -20 °C versus 40 °C ambient, both at 'large' PKED and 'large' dwell cycle conditions. Specifically, this plot illustrates the impact of large PKED and dwell on battery temperature due to its high specific heat capacity. Two shaded regions indicate conditions where aging is accelerated due to overly high (>35 °C) or overly low (<15 °C) temperatures. During the conditioning cycle, the active TMS operation pulls the battery to the intermediate temperature range for reduced aging, 15 °C to 35 °C; therefore, larger PKED conditions cycles bring the battery temperature closer to a state that is better for the future battery aging cycles starting from this condition. Conversely, then once the conditioning cycle is complete, during the dwell period the vehicle drifts back toward the ambient temperature uncontrolled, worsening the battery state initialization for the subsequent test cycle. In this way the specific combination of PKED and dwell period during the initialization simulation act together as a preconditioning for the battery before battery aging test cycle simulations. The resulting effects of this preconditioning, in the context of the temperature-dependent battery aging, indicate a need for either increased system heating capacity for battery conditioning from the most extreme cold-soaked ambient conditions or a strategy for preconditioning when there are long dwell periods that bring the battery back to the cold or hot ambient.

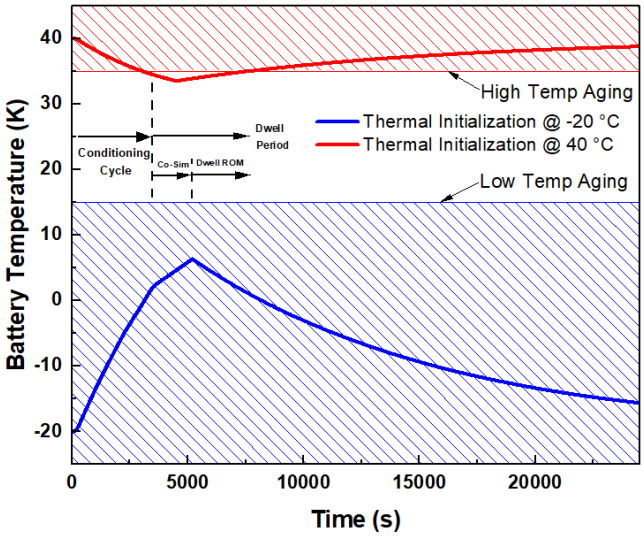

Figure 5: Thermal initialization cycles at -20 °C and 40 °C ambient conditions demonstrating the combined effects of PKED and dwell as a pre-conditioning cycle at the large bins for PKED and dwell.

With the initialization temperatures for key control volumes established by the conditioning the following battery aging test cycle simulations must calculate the distribution of current throughput across the lifetime of a typical battery

cell. This is completed first for the ambient conditions and shown in Table 4. As these are nationally averaged conditions, the majority of vehicle aging performance occurs at the 0 °C and 20 °C conditions.

Table 4: Distribution of total current throughput (Ah) for each binned temperature.

Irr\T$_{amb}$	**-20 °C**	**0 °C**	**20 °C**	**40 °C**
200	1.4%	26.7%	63.7%	8.3%

Finally, all that remains is to calculate the distribution of the current throughput (Ah) for each of the binned temperatures following the PKED and dwell bin weights shown in Table 5. As these conditions are the average conditions for light duty vehicles, the 'small' PKED trips and dwells dominate.

Table 5: Distribution of current throughput (Ah) based on PKED and dwell bin weights.

PKED\Dwell	**Small**	**Medium**	**Large**
Small	33.7%	13.3%	14.9%
Medium	12.1%	4.8%	5.4%
Large	8.4%	3.3%	3.7%

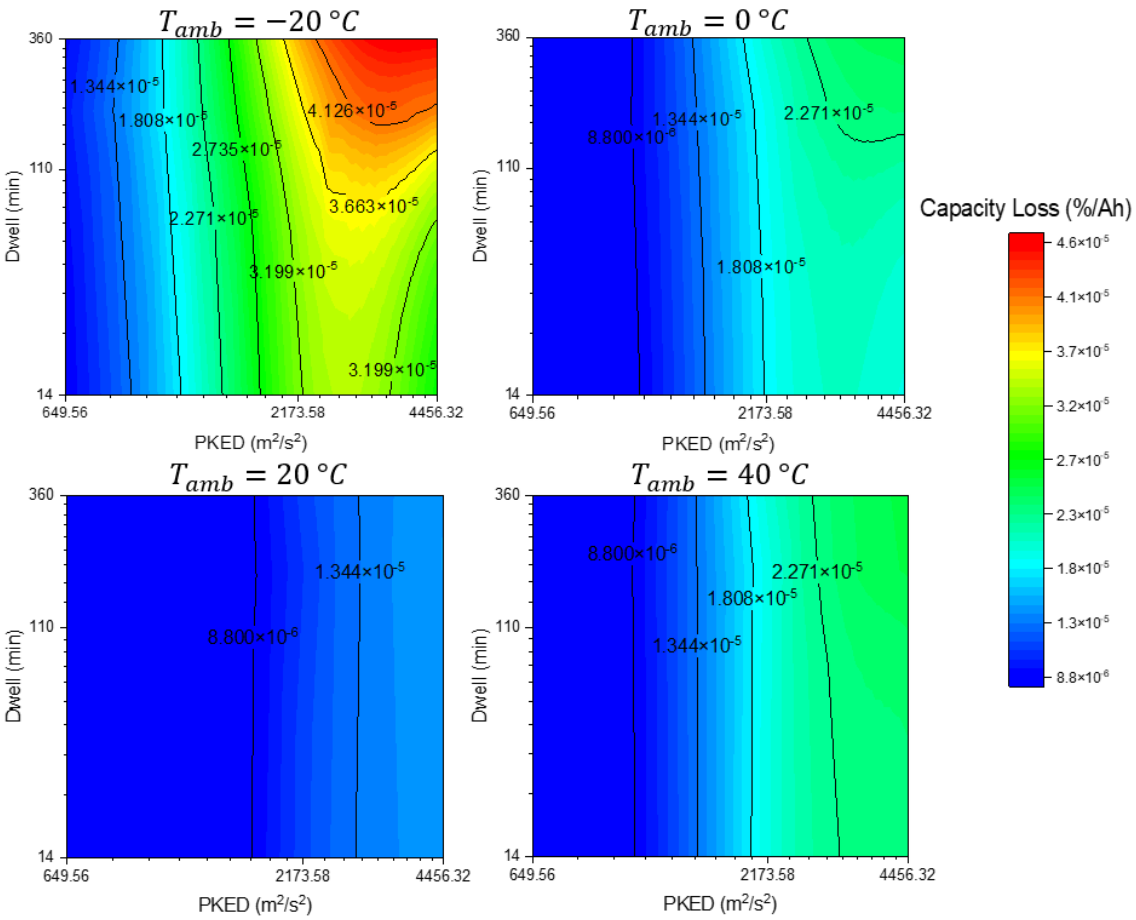

Figure 6: Contour plots of battery aging (percent aged per Ah throughput) as a function of PKED, dwell, and ambient temperature.

3.2 Battery Aging Simulations

With the thermal initialization condition solved for all combinations of PKED, dwell, and ambient condition, battery aging simulations can be completed. This works assumes linear aging of the battery beginning at a pre-aged condition of 5 kAh; this linear approach is taken because non-linear aging typically only occurs early in the battery lifetime, and if considered, the results would depend on the sequence of driving behavior considered early in battery life (e.g., whether the battery degradation started in the winter versus summer). The aging of the first cell grouping across each of these conditions is shown in Figure 6, with capacity loss defined as a percent change per amp hour throughput (%/Ah). This factor is then scaled with a linear assumption for each cell grouping to calculate aging across an assumed lifetime for the cell.

First examining the variation with ambient temperature, the expected trends are observed. There is an intermediate ambient temperature that minimizes aging at 20 °C, as this falls within the 15 °C to 35 °C sweet spot temperature range. At higher temperatures, the battery aging increases with ambient temperature that yield higher average pack temperatures which in turn accelerates the battery pack performance degradation. Similarly, at lower temperatures the battery aging decreases with temperature, with the rate of aging peaking at the minimum ambient temperature of -20 °C. Battery aging per current throughput increases with PKED, indicating that the drive cycles assumed for medium and large PKED are less efficient, which is likely due to significantly longer periods of rest during the velocity profile for medium and large PKED simulations. This should be investigated going forward with variation of the drive cycles assumed. Finally, the total aging, capacity face and power loss, of each cell grouping is shown in Table 6. Longer dwell periods increase the aging of the battery, particularly for extreme temperature conditions for which the battery can drift back to these undesirable temperatures, as discussed in the previous section. In general, the cells all reach approximately 19% capacity fade and 8% power fade at the end-of-life condition established for this study (assumed to be 25 kAh).

Table 6: Total battery aging across an assumed 25 kAh life with 5 kAh pre-aging.

Total Battery Aging	**Cell 1**	**Cell 2**	**Cell 3**	**Cell 4**	**Cell 5**	**Cell 6**
Capacity Loss (%)	18.88	19.05	19.16	19.25	19.32	19.37
Power Fade (%)	7.57	7.77	7.90	8.01	8.10	8.17

4. CONCLUSIONS

This work utilized a holistic BEV TMS model, incorporating power electronics, cabin, and battery thermal management, to predict battery aging performance as a function of PKED, dwell period, and ambient boundary conditions representative of realistic use over light duty vehicle lifetimes. The conditions considered are for national averages across the United States but the results are readily translated to a local region owing to the binning of TMY3 weather data. Based on the results from thermal initialization simulations, it is clear that ambient soaked conditions are not representative and wholly insufficient for judging lifetime behavior of battery cells. The conditioning cycle PKED and dwell period have significant effect on the pre-conditioning of key control volumes, including the battery pack. A soaked condition would drastically overpredict aging, which is most strongly a function of the battery pack temperature during the test cycle. This is seen clearly in the results for discretized battery aging for a single cell grouping and in the battery pack. Battery cell aging per amp hour throughput decreases with increasing ambient temperature up to 20 °C and begins to increase at higher temperatures. The impact of PKED and dwell pre-conditioning is that large PKED conditioning cycles and shorter dwell cycles maintain the battery closer to the TMS setpoint and therefore reduce aging. Battery aging is then successfully calculated based upon temperature and current throughput of the discretized battery module. This study also reveals several avenues future work focusing on topics including design of the battery module to improve temperature homogeneity in the pack, investigation of the effect of alternate drive cycles, and assessment of active preconditioning strategies during the dwell periods. With these investigations, battery aging can be optimized at multiple levels in view of real-world driving behavior: at the battery cell and pack levels via module construction, or at the system level with TMS design and control algorithms.

NOMENCLATURE

C	compressor	(-)
CD	charge-discharge binary value	(-)
c_p	specific heat, constant pressure	(J/kg-K)
F	fan	(-)
Irr	irradiance	(W/m^2)
P	pump or parallel	(-)
R	resistance	(ohm)
ρ	density	(kg/m^3)
S	series	(-)
T	temperature	(°C or K)
t	time	(s)
V	valve	(-)
v	velocity	(m/s)

Subscript

amb	ambient
batt	battery
flow	flow through battery module
inlet	inlet
0, 200	value for irradiance

Acronyms

BEV	battery electric vehicle
CD	charge discharge binary value
HVAC	heating ventilation and air conditioning
HX	heat exchanger
OCV	open circuit voltage
PKED	positive kinetic energy density
PTC	positive temperature coefficient
ROM	reduced order model
SOC	state of charge
TIM	thermal interface material
TMS	thermal management system
TMY	typical meteorological year
WHR	waste heat recovery

REFERENCES

Arenas, A. C., Onori, S., Guezennec, Y., & Rizzoni, G. (2015). Capacity and power fade cycle-life model for plug-in hybrid electric vehicle lithium-ion battery cells containing blended spinel and layered-oxide positive electrodes. *Journal of Power Sources, 278*, 473-483.

Cui, J., Wang, J., Weibel, J., & Pan, L. (2019). A compliant microstructured thermal interface material for dry and pluggable interfaces. *Internationl Journal of Heat and Mass Transfer, 131*, 1075-1082.

Dassault Systèmes. (2019). *What is Dymola?* Boston : Dassault Systèmes.

Du, R., Hu, X., Xie, S., Hu, L., Zhang, Z., & Lin, X. (2020). Battery aging- and temperature-aware predictive energy management for hybrid electric vehicles. *Journal of Power Sources, 473*, 228568.

IPCC. (2022). *Climate Change 2022: Impacts, Adaptation, and Vulnerability.* Cambridge: Cambridge University Press.

Jafari, M., Gauchia, A., Zhao, S., Zhang, K., & Gauchia, L. (2018). Electric Vehicle Battery Cycle Aging Evaluation in Real-World Daily Driving and Vehicle-to-Grid Services. *IEEE TRANSACTIONS ON TRANSPORTATION ELECTRIFICATION, 4*(1), 122-134.

Li, J., Huber, T., & Beidl, C. (2019). Predictive Multi-Objective Operation Strategy Considering Battery Cycle Aging for Hybrid Electric Vehicles. *SAE International Journal of Alternative Powertrains, 7*(3), 217-232.

Moniot, M., Baker, C., Lustbader, J., Lee, B., Fink, J., & Agnew, S. (2021). A framework for characterizing the initial thermal conditions of light-duty vehicles in response to representative utilization patterns, ambient conditions, and Vehicle Technologies. *SAE International Journal of Passenger Cars - Mechanical Systems*, 21-39.

Moniot, M., Lustbader, J., Wood, E., Lee, B., Fink, J., & Agnew, S. (2021). A framework for characterizing the ambient conditions experienced by light duty vehicles in the United States. *International Journal of Sustainable Transportation*, 137-151.

Shelly, T. J., Weibel, J. A., Ziviani, D., & Groll, E. A. (2020). A Dynamic Simulation Framework for the Analysis of Battery Electric Vehicle Thermal Management Systems. *19th IEEE Intersociety Conference on Thermal and Thermomechanical Phenomena in Electronic Systems (ITherm).* Orlando.

Shelly, T. J., Weibel, J. A., Ziviani, D., & Groll, E. A. (2021). Comparative analysis of battery electric vehicle thermal management systems under long-range drive cycles. *Applied Thermal Engineering, 198*, 117506.

Shelly, T., Weibel, J. A., Ziviani, D., & Eckahrd, G. A. (2021). Evaluation of Heat Pumping and Waste Heat Recovery for Battery Electric Vehicle Thermal Management. *International Refrigeration and Compressors Conference*, (p. 2219).

Shelly, T., Weibel, J. A., Ziviani, D., & Groll, E. A. (2022). A Dynamic Co-Simulation Framework for the Analysis of Battery Electric Vehicle Thermal Management Systems. *19th IEEE Intersociety Conference on Thermal and Thermomechanical Phenomena in Electronic Systems (ITherm).* San Diego: IEEE.

Titov, G., & Lustbader, J. (2017). Modeling control strategies and range impacts for electric vehicle integrated thermal management systems with MATLAB/Simulink. *SAE Technical Paper*(2017-01-0191). doi:doi:10.4271/2017-01-0191.

Titov, G., & Lustbader, J. A. (2017). Modeling Control Strategies and Range Impacts for Electric Vehicle Integrated Thermal Management Systems with MATLAB/Simulink. *SAE Technical Paper Series*.

TLK-Thermo GmbH. (n.d.). *TLK-Thermo – Engineering Services and Software for Thermal Systems*. (TLK-Thermo GmbH) Retrieved 1 07, 2020, from https://www.tlk-thermo.com/index.php/en/

VTO. (2021). *2021 Vehicle Technologies Office annual merit review report Chapter 4: Electrification.* U.S. Department of Energy.

Yu, B., Yang, J., Wang, D., Shi, J., & Chen, J. (2019). Energy consumption and increased EV range evaluation through heat pump scenarios and low GWP refrigerants in the new test procedure WLTP. *International Journal of Refrigeration, 100*, 284-294.

Zhang, Z., Wang, J., Feng, X., Chang, L., Chen, Y., & Wang, X. (2018). The solutions to electric vehicle air conditioning systems: A review. *Renewable and Sustainable Energy Reviews, 91*, 443-463.

ACKNOWLEDGEMENT

Financial support for this work provided by members of the Cooling Technologies Research Center, a graduated National Science Foundation Industry/University Cooperative Research Center at Purdue University, is gratefully acknowledged. The authors would like to acknowledge members of the Technical University of Braunschweig, Michael Steeb and Ingo Frohböse, for their support in providing access to the Modelica libraries.